# Kinetics and mechanisms of pH-dependent degradation of halonitromethanes by UV photolysis

**ARTICLE** *in* WATER RESEARCH · DECEMBER 2012

Impact Factor: 5.53 · DOI: 10.1016/j.watres.2012.11.050 · Source: PubMed



**3 AUTHORS**, INCLUDING:

Jingyun Fang
Sun Yat-Sen University
**23** PUBLICATIONS **418** CITATIONS
SEE PROFILE

Li Ling
The Hong Kong University of Science and T…
**2** PUBLICATIONS **7** CITATIONS
SEE PROFILE

Available online at www.sciencedirect.com

SciVerse ScienceDirect

journal homepage: www.elsevier.com/locate/watres

# Kinetics and mechanisms of pH-dependent degradation of halonitromethanes by UV photolysis

*Jing-Yun Fang, Li Ling, Chii Shang**

*Department of Civil and Environmental Engineering, The Hong Kong University of Science and Technology, Clear Water Bay, Kowloon, Hong Kong*

ARTICLE INFO

*Article history:*
Received 29 August 2012
Received in revised form
21 November 2012
Accepted 26 November 2012
Available online xxx

*Keywords:*
Disinfection by-products
Halonitromethane
UV photolysis
Chlorination
Bromide

ABSTRACT

Halonitromethanes (HNMs) are one of the most toxic groups of disinfection by-products. The pH-dependent degradation kinetics and pathways of four HNMs, namely bromonitromethane (BNM), dichloronitromethane (DCNM), dibromonitromethane (DBNM) and trichloronitromethane (TCNM), by ultraviolet (UV) photolysis at 254 nm were studied at pH 3–9. The UV photolysis in a dilute aqueous solution followed first-order kinetics. The photolysis rates of all four HNMs were low at pH 3–5, while that of TCNM was low at all pHs tested. Nevertheless, the photolysis rates of BNM, DCNM and DBNM increased with increasing pH, showing sharp increases as the pH neared their $pK_a$ values. The increases were correlated with their pH-dependent molar absorptivities, which were determined by the sizes of their deprotonated fractions. Homolysis was likely to be the major photolysis pathway for all four HNMs to produce halides, nitrite and nitrate at acidic pHs when the HNMs were not deprotonated. At high pHs, however, the conjugation systems of the deprotonated mono- and di-HNMs made heterolysis possibly the dominant pathway for the formation of carbon dioxide, nitrite and halides as major products for di-HNMs, and the formation of nitrite, halides and other unknown organics for mono-HNMs. The UV energy required for a 50% degradation of deprotonated HNMs in the real water sample was similar to that needed in UV disinfection processes, suggesting the effectiveness of UV photolysis in controlling HNMs that form conjugation systems at neutral to alkaline pHs.



## 1. Introduction

Halonitromethanes (HNMs) are emerging nitrogenous disinfection by-products (N-DBPs) frequently found in drinking water (Krasner et al., 2006), wastewater (Krasner et al., 2009), and swimming pool water (Liviac et al., 2010). Nine HNMs have been identified, including mono-, di- and tri-halogenated species. These HNMs are trichloronitromethane (chloropicrin, TCNM), bromodichloronitromethane (BDCNM), chloro dibromonitromethane, tribromonitromethane (bromopicrin), dichloronitromethane (DCNM), bromochloronitromethane (BCNM), dibromonitromethane (DBNM), chloronitromethane (CNM), and bromonitromethane (BNM). Results of the U.S. Nationwide DBP Occurrence Study revealed a range of concentrations for individual HNMs of 0.1–5 μg/L (Weinberg et al., 2002). The sums of analyzed HNMs represented 3% and 1% of trihalomethanes (THM4) on a median basis in national-wide surveys in the U.S. in 2000–2002 and 2006–2007, respectively (Bond et al., 2011). Among all HNM species commonly found in drinking water, TCNM is the most frequently occurring one, followed by CNM, DCNM, BDCNM and BCNM in that order (Weinberg et al., 2002; Richardson et al., 2007). The cytotoxicity and genotoxicity to Chinese hamster ovary (CHO) cells of the bromine-containing HNMs is

* *Corresponding author*. Tel.: +852 2358 7885; fax: +852 2358 1534.
E-mail address: cechii@ust.hk (C. Shang).

0043-1354/$ – see front matter © 2012 Elsevier Ltd. All rights reserved.
http://dx.doi.org/10.1016/j.watres.2012.11.050

generally higher than that of the chlorine-containing HNMs, with DBNM being the most toxic one (Plewa et al., 2004).

The formation of HNMs has been reported to be associated with chlorination and chloramination of natural organic matter, effluent organic matter, algal materials, amino acids, aliphatic amines and human sweat and urine in pool water (Hu et al., 2010a; Fang et al., 2010; Shah and Mitch, 2012). The presence of bromide could cause HNM species to transform into bromine-containing HNMs (Richardson et al., 1999). Precursor control may not be a feasible option because some of the precursors of HNMs are hard to remove by conventional coagulation, flocculation, sedimentation, filtration and adsorption processes, due to their hydrophilic nature (Westerhoff and Mash, 2002; Hu et al., 2010a; Bond et al., 2011). Therefore, post-treatment to degrade HNMs may be required in the point-of-use water treatment at the community level or even at the household level.

HNMs can be degraded by hydroxyl radicals (•OH) and hydrated electrons ($e^-_{aq}$) with rate constants of $10^7$–$10^8$ $M^{-1}$ $s^{-1}$ and 2.2–3.3 × $10^{10}$ $M^{-1}$ $s^{-1}$, respectively, at pH 7 (Mezyk et al., 2006). Hydroxyl radicals can react with TCNM to form an adduct, whose C–N bond is subsequently cleaved. Hydrated electrons react with HNMs via dissociative electron attachment to give carbon-centered radicals, followed by the release of halide and/or nitrite ions (Mezyk et al., 2006; Cole et al., 2007; Mincher et al., 2009). However, the degradation of HNMs by hydroxyl radical-based technologies is not very efficient, considering that the common advanced oxidation processes can only achieve hydroxyl radical concentrations of $10^{-14}$–$10^{-12}$ M and hydroxyl radical scavengers are often present in real water (von Gunten, 2003). Although hydrated electrons are much more efficient in degrading HNMs, they are often taken up by dissolved oxygen in water (Buxton et al., 1988). Ultrasound, a highly energy-intensive technique, degraded 99% of a 10 μM TCNM solution with recovery percentages of chloride and inorganic nitrogen (sum of $NO_3^-$ and $NO_2^-$) of 72 ± 1 and 91 ± 2%, respectively (Zhang and Hua, 2000). TCNM can also be reduced by iron or zero-valent iron with nitromethane as the intermediate and methylamine and chloride as final products (Pearson et al., 2005; Lee et al., 2008). Xenon light (a solar simulator) degraded 1 mM TCNM to $CO_2$, $Cl^-$, $NO_3^-$, and $NO_2^-$ with a half-life of 31.1 h at pH 7 and 25 °C (Wilhelm et al., 1996), which is too long to be considered effective. Solar photolysis degraded aqueous BNM, DCNM and TCNM with half-lives ranging from ~1 h–8 h (Chen et al., 2010).

UV photolysis is here proposed as a post-treatment solution that can be added to the existing treatment schemes or used in point-of-use water purification devices to control HNMs. UV photolysis has been investigated as a post-treatment means in the control of inorganic chloramines in swimming pool water (Li and Blatchley, 2009), which may be useful for controlling HNMs as well. UV photolysis has also been investigated for the removal of some emerging contaminants including pharmaceutical compounds (Pereira et al., 2007; Canonica et al., 2008), endocrine disrupting compounds (Rosenfeldt and Linden, 2004), N-nitrosodimethylamine (Sharpless and Linden, 2003), and other micropollutants (Canonica et al., 2008). However, less/little is known about whether it could be used for the removal of halogen-containing nitrogenous compounds. UV photolysis of TCNM in the gas phase has been considered as a slow process in which phosgene and nitrosyl chloride are produced (Castro and Belser, 1981). However, the degradation kinetics, products and pathways of TCNM and other HNMs during UV photolysis in the aqueous phase are unknown. The fact that mono- and di-HNMs, unlike TCNM, sharing the similar structure with that of the compounds such as nitromethane, monochloronitromethane and dinitromethane, possess acid–base properties in aqueous solution adds another layer of complexity to the problem.

The objectives of this study were 1) to examine the degradation kinetics of different HNMs by UV (254 nm) photolysis at different pHs and to correlate the pH-dependency with their chemical properties, and 2) to explore the HNM degradation products and pathways. BNM, DCNM, DBNM and TCNM were selected to represent mono-, di- and tri-HNMs.

## 2. Materials and methods

### 2.1. Chemicals

Solutions were prepared from reagent-grade chemicals and ultrapure water (18.2 MΩ cm) purified using a NANOpure system (Barnstead). BNM (>90% pure) was purchased from Aldrich. DCNM (>95% pure) and DBNM (>90% pure) were purchased from New Westminster (Canada). TCNM (>98% pure) was purchased from Chem Service (USA). The stock solutions (~1 mM) of HNMs were prepared by adding the pure compounds into ultrapure water and stirring overnight. A formaldehyde standard solution (1 mg/mL) was purchased from AccuStandard Inc. Phosphate buffers were prepared by mixing different ratios of phosphoric acid, potassium dihydrophosphate, and sodium hydrophosphate together to achieve pH 3–9.

### 2.2. UV irradiation

UV irradiation was carried out with a bench-scale collimated-beam UV irradiator, which is basically made up of four low-pressure, Hg UV lamps (254 nm, G15T8, 10 W, Sankyo Denki) housed inside a shuttered box, with a collimated tube extending from the bottom. A 250-mL sample with a water depth of 5 cm was placed in a reactor each time and the reactor was placed below the collimated tube for UV treatment, with a quartz cap (to reduce volatilization of HNMs) and rapid mixing provided at 22 ± 2 °C. The incident irradiance at 254 nm received in the reactor was 0.323 μE $L^{-1}$ $s^{-1}$ (0.153 W $L^{-1}$ $s^{-1}$) determined in a separate experiment involving the measurement of the production rate of $I_3^-$ using iodide/iodate chemical actinometry (Rahn, 1997).

### 2.3. Experimental procedures

A 250-mL solution spiked with one species of HNM at 2 μM (UV absorbance through the depth of the reactor ≤0.04) and buffered at a certain pH was subjected to UV irradiation. Samples were collected at predetermined time intervals, and then

Please cite this article in press as: Fang, J.-Y., et al., Kinetics and mechanisms of pH-dependent degradation of halonitromethanes by UV photolysis, Water Research (2012), http://dx.doi.org/10.1016/j.watres.2012.11.050

extracted with methyl t-butyl ether after adjusting the solution pH to around 4 (through addition of 5-M $H_2SO_4$). They were then subjected to the analysis of HNMs. In parallel batches, tests were conducted at initial HNM concentrations of 20 μM to determine the concentrations of halides (i.e., chloride and bromide), nitrite and nitrate as well as the final HNM concentrations. Another set of tests were conducted in a 100-mL solution spiked with DCNM of 50 μM to determine its time-dependent mineralization, the formation of organic products such as formaldehyde after UV photolysis, and the DCNM's final concentrations. Control tests of HNM hydrolysis in the dark were conducted in headspace-free bottles. The results show that the concentrations of all the four HNMs remained unchanged in 3 h at all test pHs in the dark. The result indicates that the hydrolysis of HNMs can be ignored in the time scale of our photolysis tests. All the tests were at least duplicated. The error bars in the plots represent the maximum and minimum of the experimental data of the duplicated test results.

### 2.4. Analyses

Analyses of HNMs were carried out on a gas chromatography (GC) system (Agilent 7890) coupled with a mass spectrometer (MS) using electron ionization (Agilent 5975C) according to the methods proposed by Plewa et al. (2004). The column used was a DB-17MS fused silica capillary column (with inner dimensions of 30 m × 0.25 mm and a film thickness of 0.25 μm, J&W Scientific). The GC temperature program consisted of an initial temperature of 30 °C for 10 min, followed by ramping up to 170 °C at 40 °C/min, which was held for 7 min. An injection port temperature of 170 °C and a GC–MS transfer line temperature of 210 °C were used to prevent thermal decomposition of HNMs (Chen et al., 2002). Ions at 93 and 95 a.m.u. for BNM, at 83, 85, 87, 48 and 50 a.m.u. for DCNM, at 171, 173, 175, 92, 94, 79 and 81 a.m.u. for DBNM, and at 117, 119, 121, 82 and 47 a.m.u. for TCNM were monitored. The peak heights at 95, 83, 173 and 117 a.m.u. were used to quantify BNM, DCNM, DBNM and TCNM, respectively.

The molar absorptivities ($\varepsilon_\lambda$) of each HNM at different pHs were determined by spiking ultrapure water (buffered at a certain pH) with one species of HNM at a time at levels ranging from 50 μM to 150 μM, and the UV absorbance of that HNM was determined (between 200 and 500 nm) using a UV–vis spectrophotometer (Lambda 25, Perkin Elmer) after subtraction of the UV absorbance from the buffer matrix. The $pK_a$ values of BNM, DBNM and DCNM were determined by their UV absorbance at a single wavelength of UV–vis absorbance spectra at pH 3.0–9.0 according to Boreen et al. (2004).

Total organic carbon (TOC) was quantified with a TOC analyzer (TOC-$V_{CPH}$, Shimadzu) and pH was measured with a pH meter (420-A, ORION). Concentrations of bromide, chloride, nitrite and nitrate ions were measured with a reagent-free ion chromatography (IC) system (ICS-3000, Dionex) with an injection volume of 250 μL. A high-capacity hydroxide-selective (4 × 250 mm, AS19, Dionex) analytical column and its corresponding guard column (4 × 50 mm, AG19, Dionex) were used for separation. Formaldehyde was determined using the GC system (Agilent 7890) with an electron capture detector after the derivatization/extraction procedure adopting 2,3,4,5,6-pentafluorobenzylhydroxylamine (PFBHA)/hexane according to USEPA method 556 (Munch et al., 1998). The detailed procedure for the determination of formaldehyde can be found in Text S1.

## 3. Results and discussion

### 3.1. Degradation kinetics of HNMs by UV photolysis

The photolytic degradation of BNM, DBNM, DCNM and TCNM in the diluted aqueous solution all followed the first-order kinetics, as shown in Fig. S1. Fig. 1 shows the apparent first-order degradation rate constants ($k_{app}$, $min^{-1}$) of BNM, DBNM, DCNM and TCNM by UV photolysis as a function of pH. As shown, all four HNMs degraded slowly at pH 3–5. The first-order rate constants of BNM, DBNM and DCNM increased with increasing pH, and sharp increases were observed for DBNM and DCNM as pH increased from 5 to 7 and for BNM as pH increased from 6 to 8. The largest photolysis rate constants of BNM, DBNM and DCNM were obtained at pH 9, which were 55, 14 and 98 times, respectively, higher than those at pH 4. On the other hand, the degradation of TCNM remained slow at all pHs tested. It should be noted that, in the absence of UV irradiation, the concentrations of all four HNMs remained unchanged at all pHs.

### 3.2. UV absorptivities of HNMs

The UV absorptivity of a given compound determines its amenability to direct UV photolysis and photochemical transformation. The UV–vis spectra of the four HNMs were recorded. Fig. 2 shows the corresponding molar absorptivities of HNMs in the wavelength range of 200–500 nm at different pHs. The molar absorptivities of BNM, DBNM and DCNM were strongly pH-dependent, while that of TCNM was slightly affected by pH. At pH 3–5, DCNM showed a shoulder peak spanning wavelengths 200–205 nm, while at pH 6–9 it displayed a feature peak spanning wavelengths 220–290 nm with

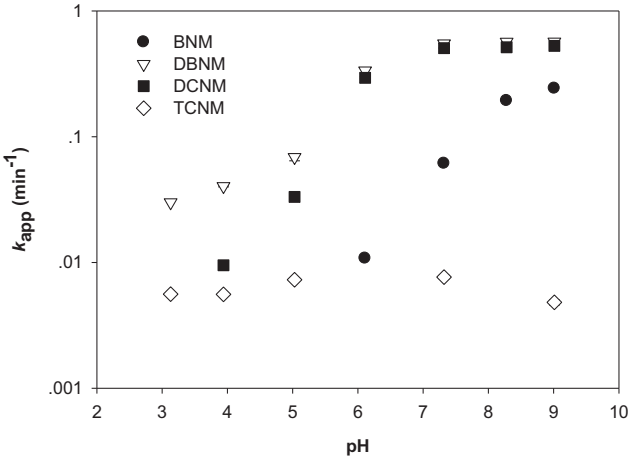


**Fig. 1 – Apparent first-order degradation rate constants ($k_{app}$) of BNM, DCNM, DBNM and TCNM as a function of pH by UV photolysis at 254 nm. All experiments were conducted with a UV irradiance of 0.153 W $L^{-1}$ and an initial HNM concentration of 2 μM at 22 ± 1 °C.**

Please cite this article in press as: Fang, J.-Y., et al., Kinetics and mechanisms of pH-dependent degradation of halonitromethanes by UV photolysis, Water Research (2012), http://dx.doi.org/10.1016/j.watres.2012.11.050

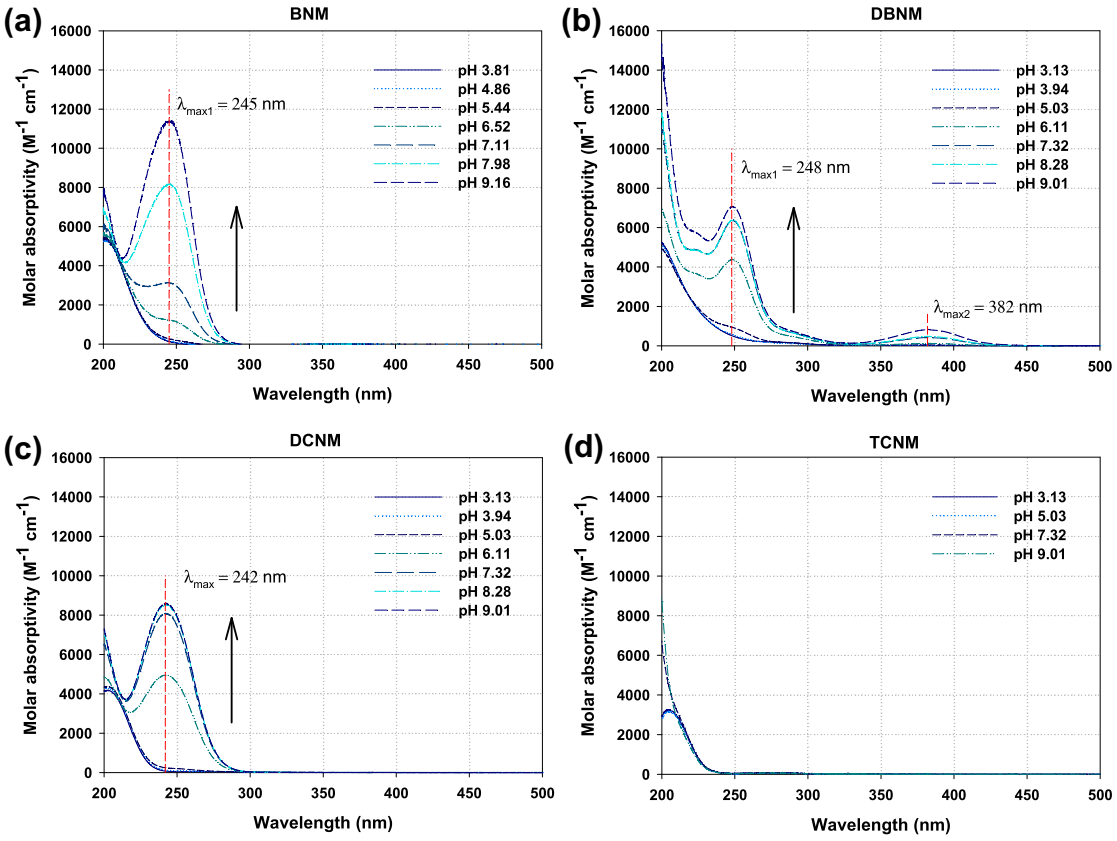


**Fig. 2 – Molar absorptivities of BNM, DBNM, DCNM and TCNM at pH values ranging from 3 to 9.**

the midpoint located at 242 nm. The height of the peak centered at 242 nm increased intensely as pH increased from 5 to 7, and then it increased further but gradually as pH increased from 7 to 9. The UV–vis spectra of BNM and DBNM, which share similar trends to that of DCNM, showed no characteristic peak at pH 3–5, but a characteristic peak centered at 248 nm for DBNM and at 245 nm for BNM at pH 6–9. The height of the characteristic peak of DBNM increased sharply as pH increased from 6 to 7, while that of BNM did the same as pH increased from 7 to 8. These characteristic peaks centered around 240–250 nm should be attributable to the $\pi \rightarrow \pi^*$ electron transition, which indicates the presence of a conjugation system in BNM, DBNM and DCNM at around neutral and alkaline pHs (McMurry, 2008). Correspondingly, the molar absorptivity of DCNM at 254 nm increased from 28 $M^{-1}$ $cm^{-1}$ to 7151 $M^{-1}$ $cm^{-1}$ as pH increased from 3 to 9, while those of DBNM and BNM increased from 378 $M^{-1}$ $cm^{-1}$ to 6524 $M^{-1}$ $cm^{-1}$ and from 39 $M^{-1}$ $cm^{-1}$ to 9764 $M^{-1}$ $cm^{-1}$, respectively. Interestingly, the molar absorptivity of DBNM at 254 nm was higher than those of DCNM and BNM at pH 3–5, but was slightly lower at pH 6–9. On the other hand, the UV spectrum of TCNM displayed only a characteristic peak centered at 208 nm and it changed little between different pHs.

### 3.3. *Linking acid–base properties of HNMs with their UV photolysis kinetics*

Shifts of UV–vis absorption peaks of mono- and di- HNMs with varying pH reflect their structural changes. As mentioned in the introduction, we speculated that mono- and di- HNMs share the similar structure with that of the organic acids such as nitromethane, monochloronitromethane and dinitromethane, which are organic acids with $pK_a$ of 10.21, 7.0 and 3.57, respectively (McMurry, 2008). So, the variation of UV–vis absorption spectra of mono- and di- HNMs can be due to their deprotonation at higher pHs, because of their acid–base properties.

The $pK_a$ values of BNM, DBNM and DCNM were determined through a spectrophotometric titration. The absorbance and pH of the solutions were used to determine the $pK_a$ values by fitting the data to eq (1) (Boreen et al., 2004):

$$x_{HNM}\varepsilon_{HNM} + x_{HNM^-}\varepsilon_{HNM^-} = \varepsilon_{tot} \quad (1)$$

where $x_{HNM}$ and $x_{HNM^-}$ are the fraction of protonated and deprotonated HNMs, respectively, and $\varepsilon$ is the molar absorptivity at specific wavelength. The $pK_a$ values of the BNM, DBNM and DCNM were determined to be 7.56 ± 0.03, 6.08 ± 0.26 and 5.97 ± 0.05, respectively (shown in Table 1), according to the absorption spectra at a single wavelength of 245 nm, 248 nm and 242 nm, respectively.

As the deprotonated fractions in solution of the three HNMs increased with increasing pH, so did their molar absorptivities near 254 nm and photodegradation rates (Figs. 1 and 2), indicating that the UV photolysis of the HNMs was mainly driven by the deprotonated fraction possessing a $\pi \rightarrow \pi^*$ conjugation system of a higher molar absorptivity. As shown in Table 1, upon deprotonation, a two-electron p-orbital on the central carbon, and the π-electron-system

Please cite this article in press as: Fang, J.-Y., et al., Kinetics and mechanisms of pH-dependent degradation of halonitromethanes by UV photolysis, Water Research (2012), http://dx.doi.org/10.1016/j.watres.2012.11.050

**Table 1 – Structures of four HNMs containing different halogen species & number and the corresponding pKa values.**

| Compound | Structure | $pK_a$ | 3D structure of protonated and deprotonated HNMs |
|---|---|---|---|
| Bromonitromethane (BNM) | 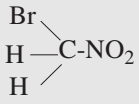 | 7.56 ± 0.03 | 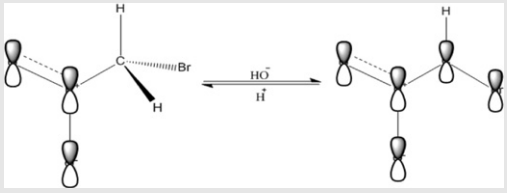 |
| Dibromonitromethane (DBNM) | 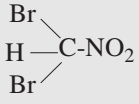 | 6.08 ± 0.26 | 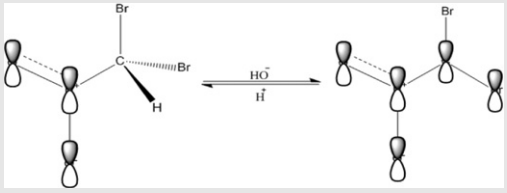 |
| Dichloronitromethane (DCNM) | 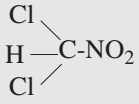 | 5.97 ± 0.05 | 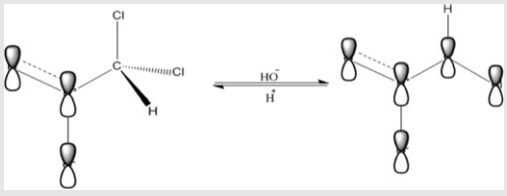 |
| Trichloronitromethane (TCNM) | 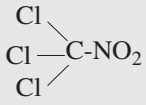 | No acid property | 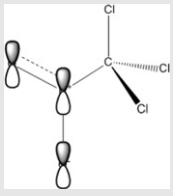 |

on the nitro group, will adopt an orientation perpendicular to the planar structure of the molecule. Taking DCNM as an example, the two-electron p-orbital overlaps with the nitro group's π-electron-system, creating a conjugation system in $Cl_2NO_2C^-$. The conjugation system decreases the energy gap between π molecular orbital and π* molecular orbital, and thus strongly absorbs UV light around 242 nm as shown by the UV absorption spectrum. This conclusion is also supported by the sharp surge in degradation rates neared the $pK_a$ of DCNM.

As for DBNM, whose conjugation system is also shown in Table 1, the trend of its photodegradation as a function of pH remains mostly similar to that of DCNM, while differences occur in two aspects: DBNM required a slightly higher pH for the sharp increase in its degradation rates to take place, and its degradation rates were much higher than those of DCNM at pH 3–5. The first difference can be explained by the relatively higher $pK_a$ of DBNM than that of DCNM due to the poorer electronegativity of bromine atoms (Atkins et al., 2006). The second difference is due to the relatively lower bond dissociation energy of the C–Br bond than the C–Cl bond (shown in Table S1) (McMurry, 2008). A lower bond dissociation energy indicates an easier bond deformation during UV treatment. Meanwhile, the UV degradation rates of BNM at all pHs tested were much lower than those of DBNM, and the sharp increase in the rates occurred at a higher pH. The relative electron withdrawing effect involving one Br atom is lower than that involving two Br atoms, which explains BNM's higher $pK_a$ and lower photo-reactivity than DBNM's.

In summary, the weak acids BNM, DBNM and DCNM dissociated into deprotonated structures accompanied by the formation of conjugation systems at neutral and basic pHs. This formation strongly increased UV absorption near 254 nm to facilitate their degradation and photochemical transformation. However, the protonated BNM, DBNM and DCNM were relatively unreactive to UV photolysis due to their much lower UV absorbances at 254 nm. TCNM lacks the acid functionality, and thus its UV spectrum and UV photolysis rates changed little with changing pH.

### 3.4. *Relationship between UV absorptivity and UV photolysis kinetics*

Fig. 3 shows the relationship between the UV absorptivities of BNM, DBNM and DCNM and their apparent first-order degradation rate constants ($k_{app}$) obtained at different pHs using the data displayed in Figs. 1 and 2. Linear relationships were

Please cite this article in press as: Fang, J.-Y., et al., Kinetics and mechanisms of pH-dependent degradation of halonitromethanes by UV photolysis, Water Research (2012), http://dx.doi.org/10.1016/j.watres.2012.11.050

found for BNM, DBNM and DCNM, with slopes of $7.29 \times 10^{-5}$, $9.15 \times 10^{-5}$ and $2.55 \times 10^{-5}$, respectively. The linearity indicates that the degradation rates of these HNMs by UV photolysis depend primarily on their UV absorptivities.

The linear relationship also indicates that the quantum yield of degradation of a specific HNM remained the same for different pHs. The quantum yield ($\Phi$) of HNM degradation by UV photolysis can be calculated using the following equation:

$$\Phi = \frac{dC/dt}{I_0 \times (1 - 10^{-\varepsilon CL})} \quad (2)$$

where $C$ is the concentration of the specific HNM, $dC/dt$ is the degradation rate of the specific HNM, $I_0$ is the UV irradiation intensity at 254 nm, $\varepsilon$ is the molar absorptivity of the HNM, and $L$ is the effective path length (5 cm in this study). As the degradation followed the first-order kinetics, the calculation of quantum yield in the diluted solution can be simplified to eq. (3) by using Taylor expansion for $10^{-\varepsilon CL}$ in the denominator of eq. (1) (details of the derivation of the eq. (3) can be found in Text S2):

$$\Phi = \frac{k_{app}}{2.303 I_0 \varepsilon L} \quad (3)$$

where $k_{app}$ is the apparent first-order degradation rate constant of the specific HNM. Thus, the slope of any specific HNM in Fig. 3 equals $2.303 I_0 L \Phi$, where $I_0 = 0.323$ μE $L^{-1}$ $s^{-1}$ and $L = 5$ cm. The quantum yields for BNM, DBNM and DCNM were calculated to be 0.114, 0.409 and 0.327, respectively. On the other hand, the quantum yield of TCNM of around $0.46 \pm 0.03$ was observed over the pH range studied (not shown). That TCNM had a higher quantum yield than DCNM can be explained by its higher degree of halogenation, which makes it less stable and more photosensitive due to the electron withdrawing effect. The same principle explains DBNM's higher quantum yield than BNM's. The quantum yield of DBNM was higher than that of DCNM with the same number of halogen substitutions, which can be attributed to the fact that the C–Br bond is less stable than the C–Cl bond.

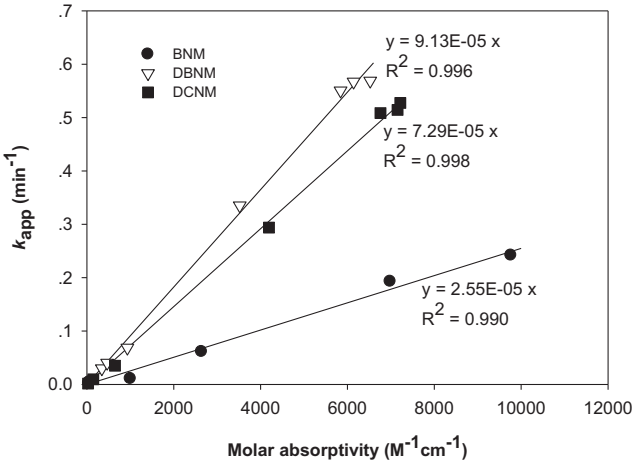


**Fig. 3 – Relationships between the UV absorptivities of BNM, DBNM and DCNM and their apparent first-order degradation rate constants ($k_{app}$) during UV photolysis at 254 nm.**

### 3.5. Degradation products and mass balances of halogen, nitrogen, and carbon

Three pH values of 3, 6 and 9 representing conditions giving different fraction sizes of deprotonated DBNM and DCNM were selected to study their ion products, and pH 6 was chosen to study TCNM with initial concentrations of HNMs of 20 μM. The anion products measured were halides, nitrite and nitrate. Fig. 4 shows the formation of halides, nitrite and nitrate and the total masses of halogen (TX, X: Cl or Br) and nitrogen (TN) during the photodegradation of DBNM, DCNM and TCNM. At pH 6 and pH 9, the major anions formed during the UV photolysis of DBNM and DCNM were halides and nitrite and their formation increased with increasing pH, while much lower quantities of nitrate (<1 μM at 20 min) were formed. At pH 3, however, halides were the major anion products, particularly for DBNM, indicating that the degradation at pH 3 was largely due to the cleavage of C–X bonds during UV photolysis. The mass balances of TX and TN (considering HNMs, halides, nitrate and nitrite only) during the photodegradation of DBNM and DCNM shared a similar trend at pH 6 and 9, with lower recovery at the initial treatment stage and higher recovery (approximately 80% nitrogen and 90% halogen) toward the end of the UV treatment, suggesting stepwise transformation of the two compounds. The higher recovery at pH 9 than pH 6 suggests faster conversion of intermediates to the final anion products at pH 9. At pH 3, the much lower recovery of TX and TN during DBNM degradation indicates the formation of unknown Br- and N-containing products other than the measured anions. The trend of the formation of anion products from BNM degradation at different pHs (i.e., pH 3, 7.5 and 9) was similar to that from DCNM and DBNM degradation (Fig. S2).

The anion products during TCNM degradation at pH 6 were tracked for 140 min, considering its slow degradation rate. The major anion formed during the UV photolysis of TCNM was chloride. Nitrite and nitrate at lower quantities were also produced. The recovery of total chlorine (TCl) and TN decreased during TCNM degradation, like it did during DBNM degradation at pH 3, suggesting the formation of some unidentified products.

The mineralization with respect to carbon (TOC reduction) and possible formation of formaldehyde during the UV photolysis of HNMs were also studied. We took DCNM as an example and conducted the tests at an initial DCNM concentration of 50 μM and pH 9. As shown in Fig. 5, the TOC concentration decreased at a slower rate than did DCNM depletion. The concentration of formaldehyde increased during DCNM degradation and reached about 5 μM after 20 min, which accounted for about 10% of the total carbon. The concentrations of other unidentified organic products (unknown org-C) (calculated by [unknown org-C] = [TOC] – [DCNM] – [formaldehyde]) increased before decreasing as UV treatment proceeded, giving a concentration of 4.3 μM after 20 min, which accounted for about 9% of the total carbon.

### 3.6. Proposed pathways of HNM degradation by UV photolysis

Degradation pathways initiated by heterolytic cleavage (Scheme 1) and homolytic cleavage (Scheme 2) of C–X bonds

Please cite this article in press as: Fang, J.-Y., et al., Kinetics and mechanisms of pH-dependent degradation of halonitromethanes by UV photolysis, Water Research (2012), http://dx.doi.org/10.1016/j.watres.2012.11.050

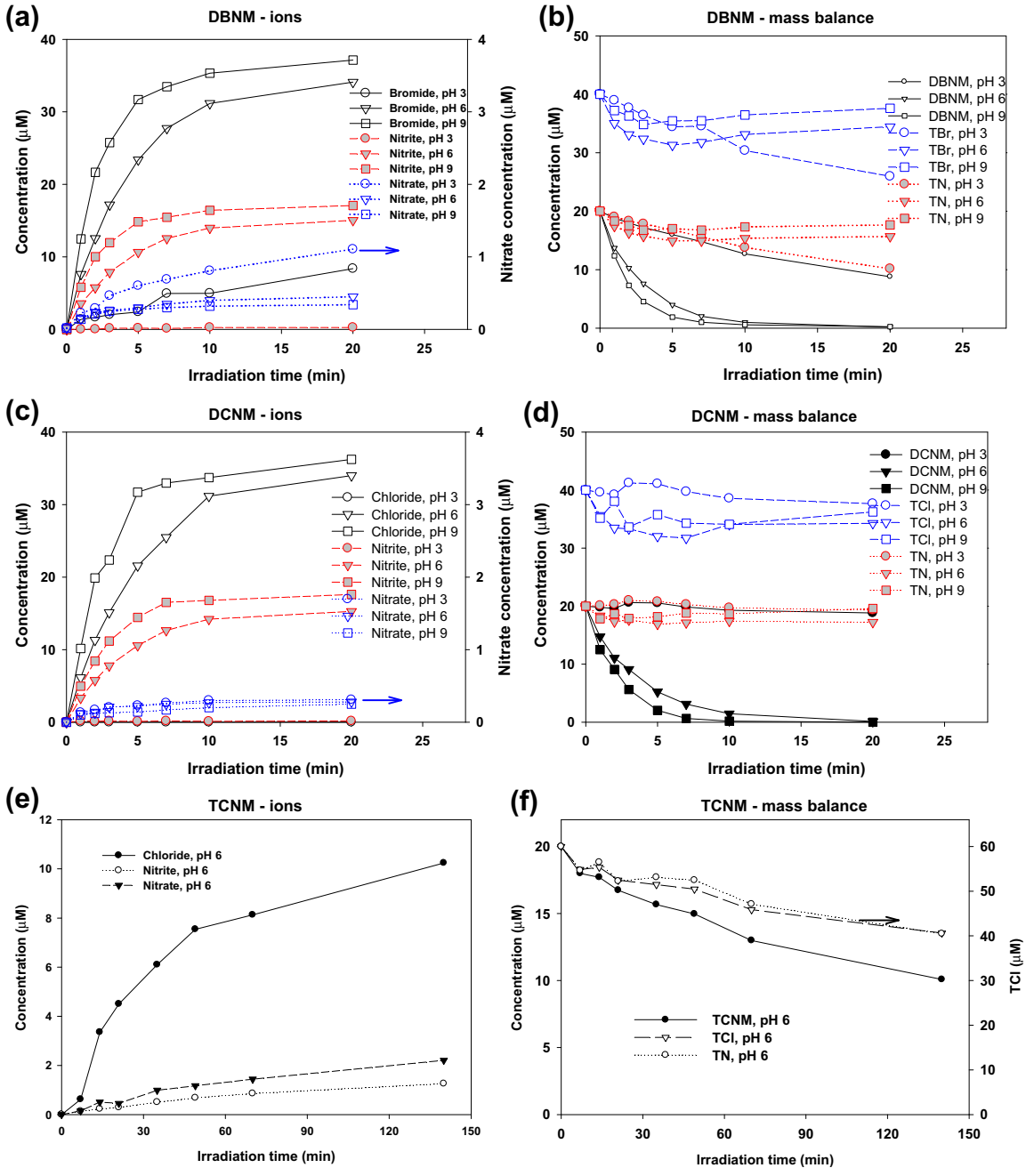


**Fig. 4 – Anion products and mass balances of total halogen (TX) and total nitrogen (TN) during DCNM, DBNM and TCNM degradation by UV photolysis at 254 nm at pH 3, 6 and 9, TX and TN were calculated by: TX = [DXNM] × 2 + [$X^-$] or TCl = [TCNM] × 3 + [$Cl^-$], TN = [HNM] + [$NO_2^-$] + [$NO_3^-$], where X represents Cl or Br. All experiments were conducted with a UV irradiance of 0.153 W $L^{-1}$ and an initial HNM concentration of 20 μM at 22 ± 1 °C.**

or C–N bonds in HNMs by UV photolysis are proposed here, based on the observed photo-products and reaction kinetics at different pHs and information available in the relative literatures (Pliego and De Almeida, 1999; Phillips et al., 2005; Cole et al., 2007; Atkins et al., 2006; McMurry, 2008). The homolytic cleavage of TCNM has been proposed in the gas phase in Castro and Belser (1981) and thus is not surprising here. However, it is interesting that the photolysis of deprotonated HNMs tends to follow the heterolytic cleavage, as discussed below.

We hypothesize that parallel reactions of heterolytic cleavages of the C–X and C–N bonds in accordance with Pathways 1 and 2 shown in Scheme 1 take place for the degradation of deprotonated HNMs ($X_2$ in Scheme 1 can be bromine or chlorine, and $X_1$ can be bromine, chlorine or hydrogen), such as BNM, DBNM and DCNM. Taking DCNM as an example, the hetero-cleavage of the C–Cl bond in $Cl_2NO_2C^-$ in Pathway 1 results in the formation of a $Cl^-$ and a chloronitrocarbene. The carbene is hypothesized to undergo rapid reactions to form either a chloronitromethanol or a

Please cite this article in press as: Fang, J.-Y., et al., Kinetics and mechanisms of pH-dependent degradation of halonitromethanes by UV photolysis, Water Research (2012), http://dx.doi.org/10.1016/j.watres.2012.11.050

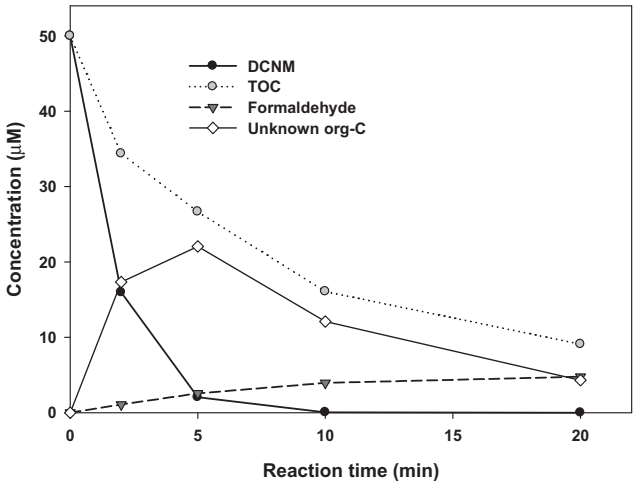


**Fig. 5 – Evolution of DCNM, TOC, formaldehyde and unidentified organic products (unknown org-C) during UV photolysis of DCNM at pH 9. [unknown org-C] = [TOC] – [DCNM] – [formaldehyde]. The experiment was conducted with a UV irradiance of 0.255 W $L^{-1}$ and an initial DCNM concentration of 50 μM at 22 ± 1 °C.**

chloronitroaldehyde, once it comes into contact with water or oxygen (Pliego and De Almeida, 1999). The formed chloronitromethanol can go through rapid hydrolysis to form $CO_2$, formaldehyde, formic acid, chloride and nitrite in the time scale of $10^{-4}$ s (Atkins et al., 2006). Fig. 4 indicates that the halogen and nitrogen atoms in the deprotonated HNMs transformed into halides and nitrite almost simultaneously during the photolysis process, due to the rapid decay of the intermediates to the final products. The pathway of deprotonated mono-HNMs is also shown in Scheme 1, where $X_2$ is Cl or Br and $X_1$ is H. Likewise, the hetero-cleavage of the C–N bond in mono- or di-HNMs as the initial step (Pathway 2) of UV photolysis may also be possible, following the similar pathways as that of the C–X bond. Pathway 1 could be favored over Pathway 2, particularly for Br-containing deprotonated HNMs, because the average bond dissociation energy is the highest for C–Br and the lowest for C–N with that for C–Cl falling somewhere in between (Table S1).

However, the homolytic cleavage pathway (Pathway 3) is hypothesized to be not favored for deprotonated HNMs, because this pathway may require a huge amount of energy (McMurry, 2008).

Scheme 2 presents the proposed homolytic cleavage of HNMs without deprotonation. In Scheme 2, X on the substrate can be chlorine, bromine, or hydrogen. The substrate is proposed to undergo either C–X bond cleavage or C–N bond

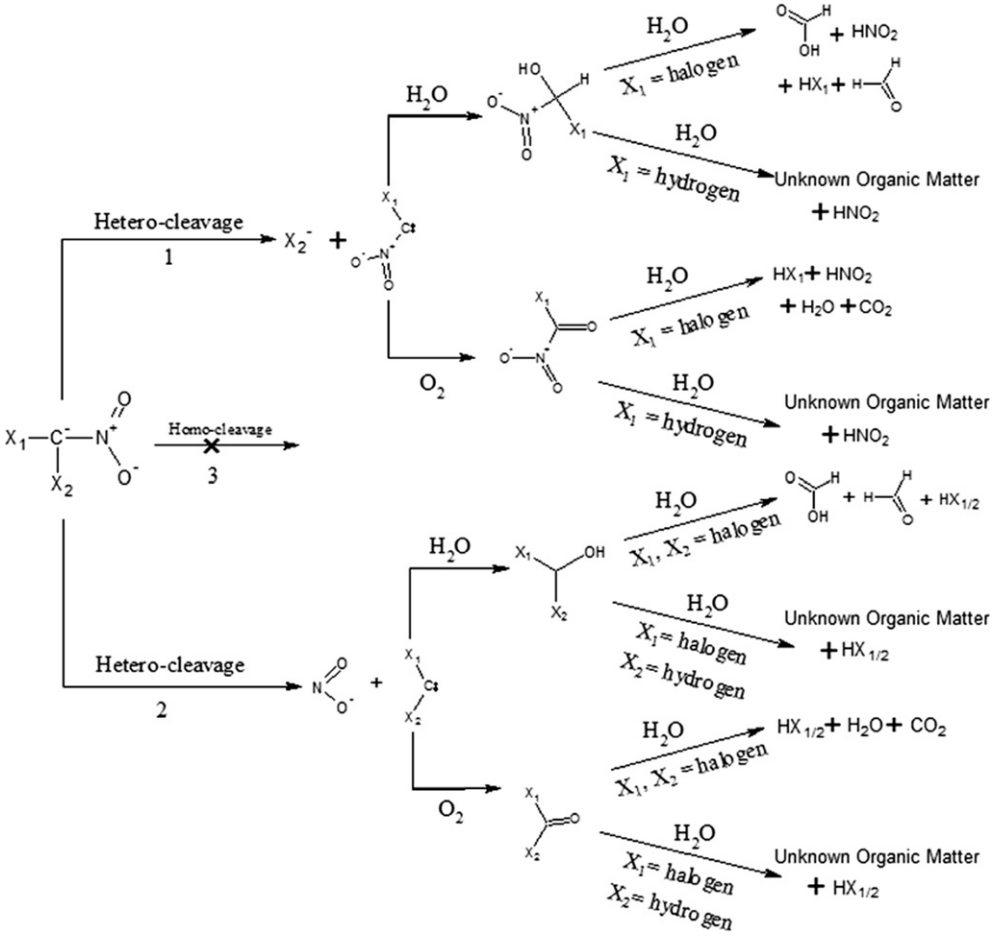


**Scheme 1 – Proposed reaction pathways for the UV photolysis of deprotonated HNMs.**

Please cite this article in press as: Fang, J.-Y., et al., Kinetics and mechanisms of pH-dependent degradation of halonitromethanes by UV photolysis, Water Research (2012), http://dx.doi.org/10.1016/j.watres.2012.11.050

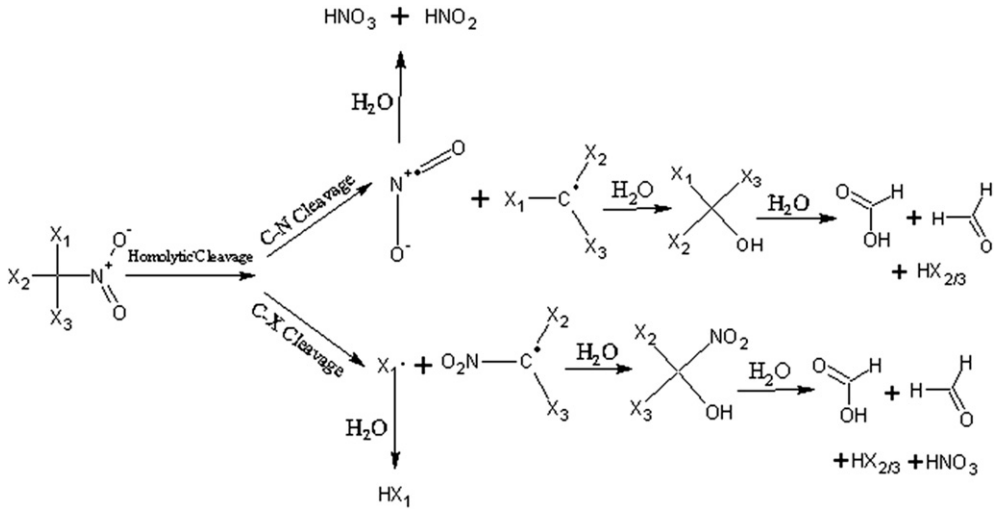


**Scheme 2 – Proposed reaction pathways for UV photolysis of HNMs without deprotonation.**

cleavage to form a halogen radical or a nitrite radical, which may react with water to produce hydrohalic acids or nitric acid and nitrous acid (Cole et al., 2007). Other radical products, $\cdot CX_3$ and $\cdot CX_2NO_2$, may react with water to produce $CX_3OH$ and $CX_2NO_2OH$, which then hydrolyze to form hydrohalic acids, nitric acid, formaldehyde, and formic acid (Phillips et al., 2005; Cole et al., 2007).

### 3.7. *HNM degradation in real water*

The degradation of DCNM, DBNM and TCNM in a real water sample: fully treated drinking water without final disinfection (the water quality is shown in Table S2) was also studied and shown in Fig. S3. As expected, the degradation of DCNM and DBNM was much faster than that of TCNM in the real water sample, with the first-order rate constants of 0.403 $min^{-1}$ and 0.419 $min^{-1}$, respectively. Also, the degradation rate constants of the three HNMs in the real water sample were all about 20% lower than those in the ultrapure water. The reduced degradation rates of HNMs in the real water sample should be primarily attributable to the presence of natural organic matter (NOM) of 1.22 mg/L with the UV absorbance at 254 nm of 0.0132 $cm^{-1}$. NOM can absorb UV light at 254 nm, so it acts as an inner filter to reduce the efficiency of HNM photolysis. The UV energy required for a 50% degradation of DCNM and DBNM was calculated to be around 80 mJ $cm^{-2}$ at neutral pH in the real water sample, which was similar to the UV energy required (40–200 mJ $cm^{-2}$) in common UV disinfection processes. However, the UV energy required for a 50% degradation of TCNM was around 70 times that required for DCNM and DBNM degradation.

## 4. Conclusions

The much higher degradation rate constants of mono- and di-HNMs than that of TCNM by UV photolysis at neutral and alkaline pHs suggest that UV photolysis is an effective post-treatment solution for controlling or even mineralizing some aqueous HNMs. In addition to BNM, DBNM and DCNM studied here, the UV photolysis should also be effective in degrading other mono- and di-HNMs such as BCNM and CNM present in deprotonated forms at near neutral pH, because these deprotonated HNMs are also expected to possess the $\pi \rightarrow \pi^*$ conjugation systems. The major products of the UV photolysis of mono- or di-HNMs at near neutral pH are halides and nitrite. Considering the reported concentrations of mono- and di-HNMs of no more than 40 nM in chlorinated drinking water (Hu et al., 2010b), the concentrations of nitrite should be insignificant.

## Acknowledgments

We gratefully acknowledge Tat-Ming Sze at the Hong Kong University of Science and Technology for his help with the experimental work, and Xu-Chun Li at Harbin Institute of Technology for his advice on UV photochemistry. This research was financially supported in part by the Research Grants Council of Hong Kong (project no. 619108).

## Appendix A. Supplementary material

Supplementary material associated with this article can be found, in the online version, at http://dx.doi.org/10.1016/j.watres.2012.11.050.

## REFERENCES

Atkins, P., Overton, T., Rourke, J., Weller, M., Armstrong, F., 2006. Inorganic Chemistry. Oxford University Press, Oxford, U.K.

Bond, T., Huang, J., Templeton, M.R., Graham, N., 2011. Occurrence and control of nitrogenous disinfection by-products in drinking water – a review. Water Research 45 (15), 4341–4354.

Boreen, A.L., Arnold, W.A., McNeill, K., 2004. Photochemical fate of sulfa drugs in the aquatic environment: sulfa drugs containing five-membered heterocyclic groups. Environmental Science and Technology 38 (14), 3933–3940.

Buxton, G.V., Greenstock, C.L., Helman, W.P., Ross, A.B., 1988. Critical-review of rate constants for reactions of hydrated electrons, hydrogen-atoms and hydroxyl radicals (.OH/.O-) in aqueous-solution. Journal of Physical and Chemical Reference Data 17 (2), 513–886.

Canonica, S., Meunier, L., von Gunten, U., 2008. Phototransformation of selected pharmaceuticals during UV treatment of drinking water. Water Research 42 (1–2), 121–128.

Castro, C.E., Belser, N.O., 1981. Photohydrolysis of methyl bromide and chloropicrin. Journal of Agricultural and Food Chemistry 29 (5), 1005–1008.

Chen, B., Lee, W., Westerhoff, P.K., Krasner, S.W., Herckes, P., 2010. Solar photolysis kinetics of disinfection byproducts. Water Research 44 (11), 3401–3409.

Chen, P.H., Richardson, S.D., Krasner, S.W., Majetich, G., Glish, G.L., 2002. Hydrogen abstraction and decomposition of bromopicrin and other trihalogenated disinfection byproducts by GC/MS. Environmental Science and Technology 36 (15), 3362–3371.

Cole, S.K., Cooper, W.J., Fox, R.V., Gardinali, P.R., Mezyk, S.P., Mincher, B.J., O'Shea, K.E., 2007. Free radical chemistry of disinfection byproducts. 2. Rate constants and degradation mechanisms of trichloronitromethane (chloropicrin). Environmental Science and Technology 41 (3), 863–869.

Fang, J., Ma, J., Yang, X., Shang, C., 2010. Formation of carbonaceous and nitrogenous disinfection by-products from the chlorination of Microcystis aeruginosa. Water Research 44 (6), 1934–1940.

Hu, J., Song, H., Addison, J.W., Karanfil, T., 2010a. Halonitromethane formation potentials in drinking waters. Water Research 44 (1), 105–114.

Hu, J., Song, H., Karanfil, T., 2010b. Comparative analysis of halonitromethane and trihalomethane formation and speciation in drinking water: the effects of disinfectants, pH, bromide, and nitrite. Environmental Science and Technology 44 (2), 794–799.

Krasner, S.W., Weinberg, H.S., Richardson, S.D., Pastor, S.J., Chinn, R., Sclimenti, M.J., Onstad, G.D., Thruston, A.D., 2006. Occurrence of a new generation of disinfection byproducts. Environmental Science and Technology 40 (23), 7175–7185.

Krasner, S.W., Westerhoff, P., Chen, B.Y., Rittmann, B.E., Amy, G., 2009. Occurrence of disinfection byproducts in United States wastewater treatment plant effluents. Environmental Science and Technology 43 (21), 8320–8325.

Lee, J.-Y., Pearson, C.R., Hozalski, R.M., Arnold, W.A., 2008. Degradation of trichloronitromethane by iron water main corrosion products. Water Research 42 (8–9), 2043–2050.

Li, J., Blatchley, E.R., 2009. UV photodegradation of inorganic chloramines. Environmental Science and Technology 43 (1), 60–65.

Liviac, D., Wagner, E.D., Mitch, W.A., Altonji, M.J., Plewa, M.J., 2010. Genotoxicity of water concentrates from recreational pools after various disinfection methods. Environmental Science and Technology 44 (9), 3527–3532.

McMurry, J., 2008. Organic Chemistry. Thomson Brooks/Cole, California, U.S.

Mezyk, S.P., Helgeson, T., Cole, S.K., Cooper, W.J., Fox, R.V., Gardinali, P.R., Mincher, B.J., 2006. Free radical chemistry of disinfection-byproducts. 1. Kinetics of hydrated electron and hydroxyl radical reactions with halonitromethanes in water. The Journal of Physical Chemistry A 110 (6), 2176–2180.

Mincher, B.J., Mezyk, S.P., Cooper, W.J., Cole, S.K., Fox, R.V., Gardinali, P.R., 2009. Free-radical chemistry of disinfection byproducts. 3. Degradation mechanisms of chloronitromethane, bromonitromethane, and dichloronitromethane. The Journal of Physical Chemistry A 114 (1), 117–125.

Munch, J.W., Winslow, D.J.M., Wendelken, S.D., 1998. U.S. EPA Method 556: Determination of Carbonyl Compounds in Drinking Water by Pentafluorobenzylhydroxylamine Derivatisation and Capillary Gas Chromatography with Electron Capture Detection. U.S. Environmental Protection Agency, Cincinnati, OHIO 45268.

Pearson, C.R., Hozalski, R.M., Arnold, W.A., 2005. Degradation of chloropicrin in the presence of zero-valent iron. Environmental Toxicology and Chemistry 24 (12), 3037–3042.

Pereira, V.J., Weinberg, H.S., Linden, K.G., Singer, P.C., 2007. UV degradation kinetics and modeling of pharmaceutical compounds in laboratory grade and surface water via direct and indirect photolysis at 254 nm. Environmental Science and Technology 41 (5), 1682–1688.

Phillips, D.L., Zhao, C., Wang, D., 2005. A theoretical study of the mechanism of the water-catalyzed HCl elimination reactions of CHXCl(OH) (X = H, Cl) and HClCO in the gas phase and in aqueous solution. The Journal of Physical Chemistry A 109 (42), 9653–9673.

Plewa, M.J., Wagner, E.D., Jazwierska, P., Richardson, S.D., Chen, P.H., McKague, A.B., 2004. Halonitromethane drinking water disinfection byproducts: chemical characterization and mammalian cell cytotoxicity and genotoxicity. Environmental Science and Technology 38 (1), 62–68.

Pliego, J.R., De Almeida, W.B., 1999. A new mechanism for the reaction of carbenes with OH groups. The Journal of Physical Chemistry A 103 (20), 3904–3909.

Rahn, R.O., 1997. Potassium iodide as a chemical actinometer for 254 nm radiation: use of iodate as an electron scavenger. Photochemistry and Photobiology 66 (4), 450–455.

Richardson, S.D., Plewa, M.J., Wagner, E.D., Schoeny, R., DeMarini, D.M., 2007. Occurrence, genotoxicity, and carcinogenicity of regulated and emerging disinfection by-products in drinking water: a review and roadmap for research. Mutation Research-Reviews in Mutation Research 636 (1–3), 178–242.

Richardson, S.D., Thruston, A.D., Caughran, T.V., Chen, P.H., Collette, T.W., Floyd, T.L., Schenck, K.M., Lykins, B.W., Sun, G.-R., Majetich, G., 1999. Identification of new drinking water disinfection byproducts formed in the presence of bromide. Environmental Science and Technology 33 (19), 3378–3383.

Rosenfeldt, E.J., Linden, K.G., 2004. Degradation of endocrine disrupting chemicals bisphenol A, ethinyl estradiol, and estradiol during UV photolysis and advanced oxidation processes. Environmental Science and Technology 38 (20), 5476–5483.

Shah, A.D., Mitch, W.A., 2012. Halonitroalkanes, halonitriles, haloamides, and N-nitrosamines: a critical review of nitrogenous disinfection byproduct formation pathways. Environmental Science and Technology 46 (1), 119–131.

Sharpless, C.M., Linden, K.G., 2003. Experimental and model comparisons of low- and medium-pressure Hg lamps for the direct and $H_2O_2$ assisted UV photodegradation of N-nitrosodimethylamine in simulated drinking water. Environmental Science and Technology 37 (9), 1933–1940.

von Gunten, U., 2003. Ozonation of drinking water: part I. Oxidation kinetics and product formation. Water Research 37 (7), 1443–1467.

Weinberg, H.S., Krasner, S.W., Richardson, S.D., Thruston Jr., A.D., 2002. The Occurrence of Disinfection By-products (DBPs) of Health Concern in Drinking Water: Results of a Nationwide DBP Occurrence Study. EPA/600/R-02/068.

Westerhoff, P., Mash, H., 2002. Dissolved organic nitrogen in drinking water supplies: a review. Journal of Water Supply Research and Technology-Aqua 51 (8), 415–448.

Environment fate of chloropicrin in fumigants: environmental fate, exposure, and analysis. In: Wilhelm, S.N., Shepler, K., Lawrence, L.J., Lee, H. (Eds.), Fumigants Environmental Fates, Analysis, Exposure. ACS Symp. Ser., vol. 652. American Chemical Society, Washington, DC.

Zhang, G.M., Hua, I., 2000. Ultrasonic degradation of trichloro acetonitrile, chloropicrin and bromobenzene: design factors and matrix effects. Advances in Environmental Research 4 (3), 211–218.

Please cite this article in press as: Fang, J.-Y., et al., Kinetics and mechanisms of pH-dependent degradation of halonitromethanes by UV photolysis, Water Research (2012), http://dx.doi.org/10.1016/j.watres.2012.11.050